# Liver-Type Fatty Acid Binding Protein (FABP1) Has Exceptional Affinity for Minor Cannabinoids

Dr. Fred Shahbazi[a,b*†], Sanam Mohammadzadeh[a†], Dr. Daniel Meister[a,b], Valentyna Tararina[a,c,d‡], Vagisha Aggarwal,[a,e,f‡] Dr. John F. Trant[a,b,g*]

†F.S. and S.M. contributed equally to this work and can order their name in any order for any professional purpose.

‡ V.T. and V.A contributed equally to this work and can order their name in any order for any professional purpose.

[a] *Department of Chemistry and Biochemistry, University of Windsor, 401 Sunset Avenue, Windsor ON, N9B 3P4, Canada*

[b] *Binary Star Research Services, LaSalle ON, N9J 3X8, Canada*

[c] *Department of Chemistry, Taras Shevchenko National University of Kyiv, 60 Volodymyrska St., Kyiv, Ukraine*

[d] *Current Affiliation: Chemspace, 85 Winston Churchill St., Kyiv, 02094, Ukraine*

[e] *Department of Applied Chemistry, Delhi Technological University, Rohini, New Delhi, Delhi, 110042, India*

[f] *Current Affiliation: Department of Chemistry, Paris Sciences & Lettres, 60 Rue Mazarine, 75006 Paris, France*

[g] *We-Spark Health Institute, Windsor, ON, N9B 3P4*

* Corresponding authors' email: farsheed@uwindsor.ca, j.trant@uwindsor.ca

**Abstract:**

Fatty acid binding protein 1 (FABP1) is a lipid transporter primarily expressed in the liver where it helps move fatty acids between lipid membranes. Inhibition of FABP1 has potential therapeutic implications for nonalcoholic fatty liver disease, metabolic syndrome & obesity, diabetes, and inflammatory & cardiovascular diseases. Curiously, FABP1 is known to bind to both endocannabinoids (ECs) and the major phytocannabinoids (PCs) with moderately high affinities. We have developed an *in-silico* model of the protein and validated it against experimental data. We then employed the model to predict the binding mode and affinities of minor cannabinoids (MCs) to FABP1. Our study predicts that the top ranked MCs **5-acetyl-4-hydroxy-CBG** and **CBGA** bind stronger than fatty acids (FAs), ECs or PCs, and participate in the key interactions used to stabilize FABP1-FA complexes. This makes them promising starting points for the

development of new therapeutics. The implications this has on considering the minor cannabinoids as low entropy isosteres of the fatty acids is also discussed.

**Keywords:** minor cannabinoids, THC, molecular modeling, ligand profiling

## Introduction

Fatty acid binding proteins transport water-insoluble hydrophobic molecules from membrane to membrane within a cell.[1] Of the ten identified members, FABP1 is the most highly expressed in humans overall, and is found primarily in tissues involved in fatty acid (FA) metabolism where it is implicated in their transport, especially to the mitochondria for oxidation.[2] It consequently regulates lipid metabolism and downstream cellular signaling pathways.[3] The mechanism of how FABP1 affects these signaling pathways is not fully understood, but might be through the PPAR pathway as the two proteins physically interact; regardless, abnormal (either elevated or decreased) levels of FABP1 are indicative of diabetic nephropathy and are predictive clinical markers of renal illnesses.[4] Knockout of the gene leads to mice with significant weight gain,[2, 5] and FABP1 overexpression enhances hepatocyte fatty acid uptake,[6] and is associated with a variety of cancers,[7] including liver, lung, stomach, and colon.

The chemical inhibition of FABP1 phenotypically modifies FA storage in adipose; this changes FA uptake, esterification, oxidation, nuclear targeting, and intracellular transport.[2] Inhibition of FABP1 fatty acid transport has been proposed as a target for preventing or reversing diet-induced obesity and diabetes.[8]

Although FABP1 is structurally related to the other FABPs, it is distinguished by its far larger binding cavity; this means that FABP1 alone can bind two FAs concurrently, and can also interact with other large hydrophobic species such as bilirubin and lysophospholipids.[9] When transporting traditional FAs, the first molecule, with affinity in the nM range, is totally encapsulated within the β-barrel structure of the protein, generally in a U-shaped conformation, locked in both by hydrophobic collapse and the carboxylate forming a series of H-bonds with **R$^{122}$** and **S$^{39}$**, and a water-bridged interaction with **S$^{124}$** (Fig. 1, black mesh surface).[8-9] The second FA binds mostly by hydrophobic forces to the "lipophilic" binding pocket in the portal region with its carboxylic group buried in the protein cavity by polar contacts with **N$^{111}$** and **R$^{122}$** (Fig. 1, blue mesh surface, PDB: *3STK*).[8, 10] This portal region can be thought of as the entry gate to the deeper pocket, but is a large enough opening that it can accommodate the second molecule. Of course, dissociation must occur first through the portal-bound molecule, followed by the high affinity bound molecule deep in the pocket. This is only really feasible when FABP1 is associated with a lipid membrane as otherwise the solvation energy is too much to overcome. Each of these two sites demonstrates similar high affinities for saturated FAs, while their affinities for polyunsaturated

fatty acids (PUFA) differs by more than 7-fold.[11] FABP1 has high affinity for *n*-6 polyunsaturated fatty acids (PUFA) such as arachidonic acid (ARA), or its endocannabinoid derivatives (ECs), anandamide (AEA), and 2-Arachidonoylglycerol (2-AG). This is because the internal site does not require a carboxylate group to attain high affinity.[10]

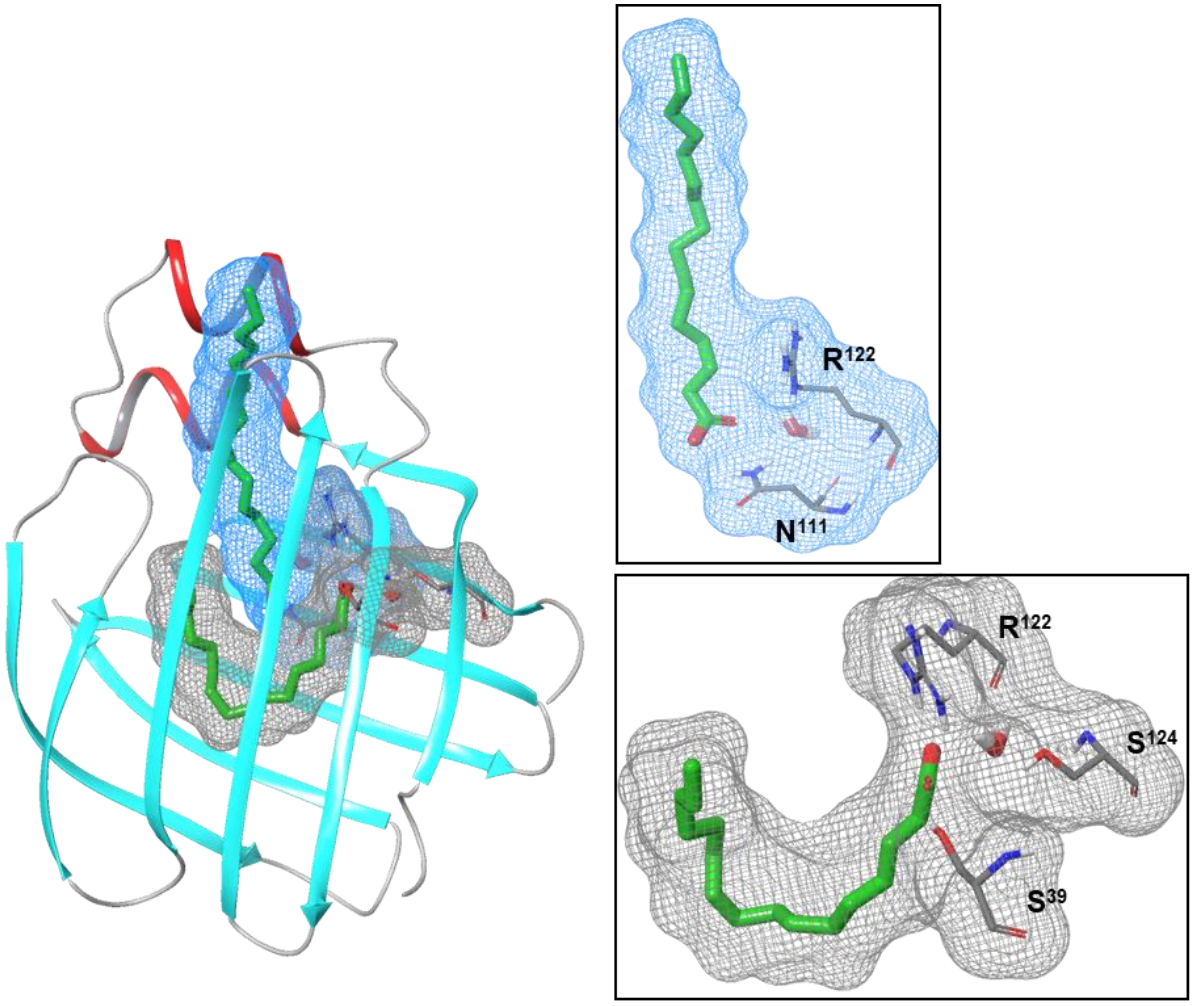


**Figure 1.** Structure of FABP1 bound to two palmitic acid residues (molecules in green, surface in blue and black mesh). The β-sheets of the protein are in cyan, the alpha helices in red. The structure is obtained following a relaxation of the crystal structure, *3STK* in an implicit water model.

In late 2019, Elmes and colleagues released the crystal structure of human FABP1 in complex with THC at 2.5Å resolution; the first crystal structure of a FABP bound to a cannabinoid (PDB: *6MP4*).[12] By promoting FABP1's cytoplasmic trafficking to hepatic CYP450 enzymes, they

showed that FABP1 plays a significant role in regulating THC biotransformation and metabolism. The large THC molecule fills the majority of the FABP1 binding cavity. Its conjugated rings occupy a hydrophobic pocket, its pyran ring's O1 atom forms a hydrogen bond with **N$^{111}$**, and its carbon chain stretches back towards the pocket entrance. The bulky THC molecule occupies the majority of the FABP1 binding cavity. To support this effort or for experimental reasons, they also acquired a comparison of THC (PDB: *6MP4*) and palmitic acid (PDB: *3STM*) both bound to FABP1; THC is located away from the fatty acid's more polar environment. THC-FABP1 lacks the ion pair interaction between the carboxylate of the FAs and **R$^{122}$**; the **M$^{74}$** sidechain moves substantially to accommodate the large THC rings in the hydrophobic pocket, while the **F$^{50}$** sidechain rotates to pack against THC's short hydrocarbon tail. However, there are significant steric clashes that are induced by the presence of THC in the binding pocket; indicating that the simultaneous binding of THC with endogenous lipids is unlikely.. Likely only one or the other can bind at any one time.

Stepping back for a moment, let us consider the structures of the two classes of cannabinoids: the endocannabinoids (EC) and the phytocannabinoids (PC, Figure 2). The ECs are structurally unrelated to the PCs: the former are long *cis*-polyunsaturated alkyl chains with a polar head group, the latter a polycyclic monoterpene-resorcinol conjugate, but both act on the cannabinoid CB1 and CB2 receptors in the brain.[13] Clearly, both also interact with FABP1. Although FABP1 is not found in the brain, it still regulates the levels of the ECs by facilitating their metabolism in the liver: FABP1 ablation preferentially elevated brain ECs system AEA and 2-AG outside of the central nervous system.[14] PCs may enhance ECs signaling by competing with FABP1 for absorption and subsequent metabolism.[12] This suggests that the endocannabinoids tend to fold, when in contact with proteins, into a compact surface reminiscent of the phytocannabinoids. As this requires a series of single bonds to all specifically rotate into a non-extended, low-dynamic conformation, there is a significant entropic cost.[15] The PCs do not have to pay this cost as the cyclic structure locks in the positioning. The fact that the endocannabinoids and the phytocannabinoids, despite their radically different structures both adopt binding conformations with the cannabinoid receptors and the unrelated FABPs points to their close conformational arrangement.

Despite the research focus, the diverse attributed bioactivity of the cannabinoids cannot be explained simply from interaction at the CB1 and CB2 receptors.[16] Some of this non-CB activity

can however, be ascribed to the FABPs. Binding to intracellular FABPs has an effect on ligand-dependent transactivation of PPARs, a receptor known to be targeted by various cannabinoids through direct activation of its orthosteric site.[17] Furthermore, occupation of FABP1 increases AEA and 2-AG levels in the liver and brain (by decreasing the rate of their metabolism). The interactions may have an impact on inducing weight gain (as seen in the mouse models), but may also be important for controlling overexpression diseases.[14] Either way, cannabinoids might prove to be useful tools for probing the biology around FABP1, but, like all cases, the major cannabinoids are likely not the most active. THC and CBD are only the most common of over 200 phytocannabinoids that have been identified in *C. sativa* extracts.[18] The minor cannabinoids are only minor relative to the major ones, as consumers of cannabis may take in gram quantity of material at a time, the minor cannabinoids can be present in sufficient enough quantity to have meaningful biological activity.[19] These minor compounds could be far more potent than the major components. However, many of these minor cannabinoids have only been isolated or identified a few times, and besides a few "trendy" compounds are not readily available. This situation implies that an *in silico* screen would potentially prove valuable as a first step.

In order to develop a useful predictive *in silico* screen, one must build a good model of the protein and derive equations that can relate quantitative computationally-derived molecular interaction strengths with an experimental readout. This requires both a well-defined structure of the target protein, and a self-consistent and broad dataset. No such complete model exists for FABP1, but the required inputs are available. We consequently began our screen of FABP1 and minor cannabinoids with the generation of a corrected 3-D structure of the protein and a mathematical model that can recapitulate known interactions with known binders. If found useful, this can then be extended to screen new molecules to prophesize affinity. Our generation and application of this model is the focus of this current report.

## Results and Discussion

A total of 18 ligands with empirically-measured binding affinity, $K_i$, for FABP1, determined using the same fluorescence displacement assay by Huang and co-workers,[14, 20] were used to inform the model. The list includes both N-Acylethanolamides (NAEs) and 2-Monoacylglycerides (2-MGs) **AEA**, **OEA**, **EPEA**, **DHEA**, **2-AG**, **2-OG** & **2-PG**, AEA uptake

Inhibitors **AM404**, **VDM11**, **OMDM1** & **OMDM2**, general preclinical FABP inhibitors **BMS309403**, **SCPI1**, **SCPI3** & **SCPI4**, and **THC**, **CBD** & synthetic cannabinoid **JWH-018** (Figure 2). We used the Ligprep feature in Maestro to prepare the structures of each ligand. We obtained the SMILES notation for each compound from PubChem and entered it into Ligprep's SMILES field for structure preparation. Based on the binding configuration observed for THC in the X-ray crystallography structure (PDB: 6MP4), we employed Schrödinger's Maestro suite of computational tools, including for RRD, IFD, MD simulations, MMGBSA calculations, root-RMSD, and H-bond analysis for computational predictions of how experimental ligands would bind to the binding site. Our goal was to determine whether the computed interaction energies would align with the experimental trends. Details on how the FABP1 structures were prepared for simulations are available in the supplementary information.

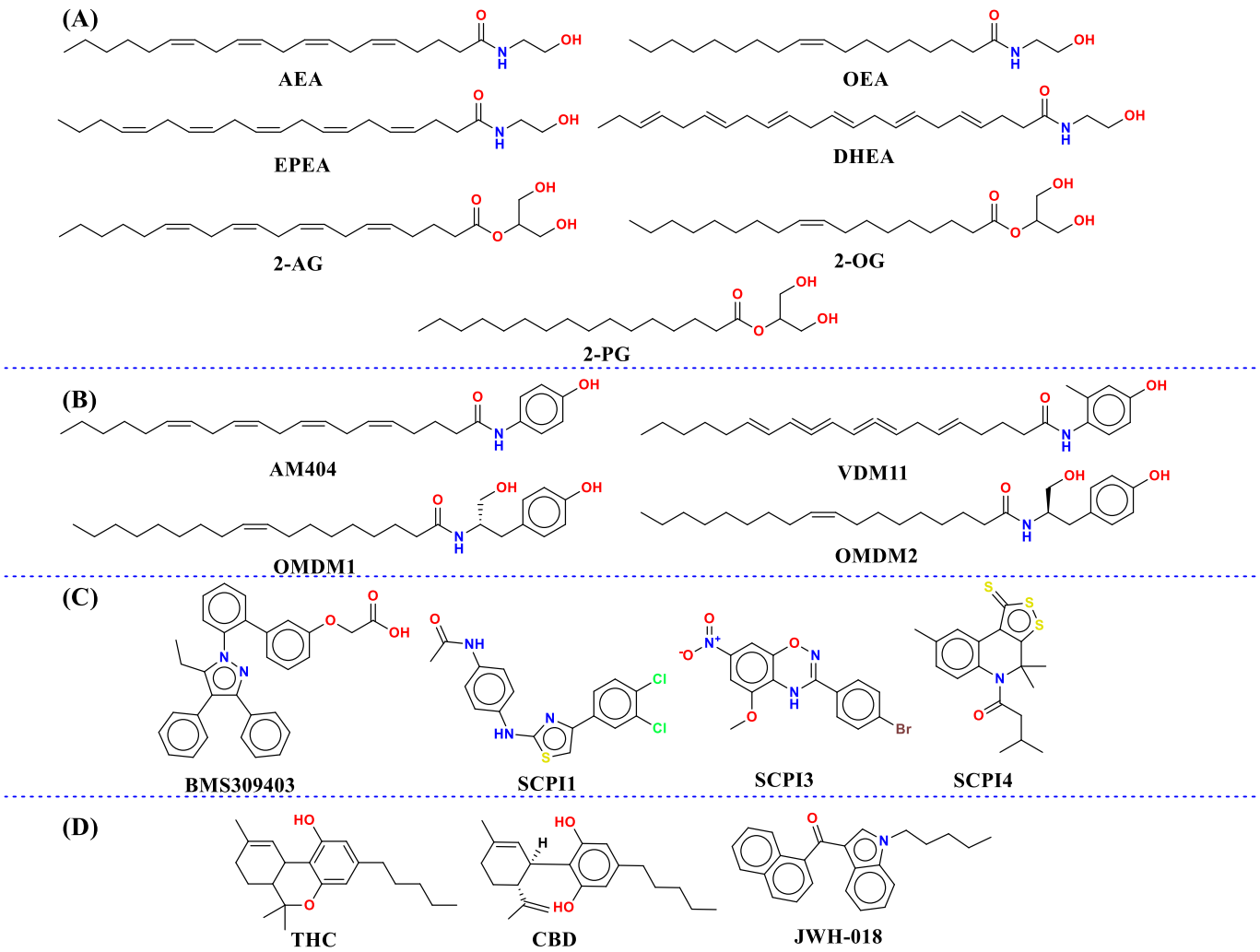


**Figure 2.** Structures of the experimental ligands with known experimental binding affinities used in this study to validate the molecular model of FABP1: A) NAEs and 2-MGs, B) AEA uptake Inhibitors, C) general FABPs inhibitor and D) phyto- and synthetic cannabinoids.

Several in-silico techniques were employed in scoping studies to create a model that gives a reliable correlation between experimental and computational data. First, rigid receptor docking (RRD) model was employed and the van der Waals radii of non-polar atoms was lowered to 0.8 to indicate some of the residue's flexibility.[21] Prime/MM–GBSA calculations were then done on this docked structure and the distance between flexible residues and ligands adjusted to 5.0 Å to better estimate the binding free energy of the most stable docked structure for each ligand.[22] Computationally more intensive induced fit docking (IFD) calculations were then performed on the top hits; IFD enables flexibility in the binding site residues and generally generates a more

reliable complex. The experimental $K_i$ values, calculated physiochemical properties, rigid docking scores (RRD 0.8), IFD and MD/MM-GBSA were collected and analyzed (Table 1).

**Table 1.** $K_i$ value, calculated physiochemical properties, RRD scores, IFD and MD/MM-GBSA of the FABP1 ligands. Experimental values were extracted from Huang and coworkers.[14, 20]

| Experimental | | | Physiochemical Properties | | | Computational (kcal/mol) | | |
|---|---|---|---|---|---|---|---|---|
| **Ligand** | **$K_i$ (nM)** | **Log ($K_i$)** | **LogP (O/W)** | **MW (g/mol)** | **PSA** | **RRD 0.8** | **IFD** | **MD/MM-GBSA** |
| **AEA** | 111 | 2.05 | 4.94 | 347.54 | 54.99 | -7.71 | -9.53 | -51.01 |
| **OEA** | 43 | 1.63 | 4.46 | 325.53 | 54.99 | -8.27 | -9.81 | -49.06 |
| **EPEA** | 390 | 2.59 | 4.62 | 345.52 | 59.15 | -9.46 | -8.78 | -48.66 |
| **DHEA** | 163 | 2.21 | 5.17 | 371.56 | 58.76 | -8.34 | -9.42 | -54.64 |
| **2-AG** | 61 | 1.79 | 5.34 | 378.55 | 79.99 | -9.30 | -9.16 | -56.76 |
| **2-OG** | 40 | 1.60 | 4.86 | 356.55 | 77.89 | -9.92 | -9.83 | -48.64 |
| **2-PG** | 70 | 1.85 | 4.14 | 330.51 | 70.56 | -8.85 | -9.50 | -50.73 |
| **AM404** | 29 | 1.46 | 6.87 | 395.58 | 57.80 | -9.23 | -12.45 | -56.32 |
| **VDM11** | 37 | 1.57 | 7.14 | 409.61 | 55.70 | -9.25 | -11.53 | -54.37 |
| **OMDM1** | 40 | 1.60 | 5.51 | 431.66 | 70.41 | -8.52 | -10.95 | -59.03 |
| **OMDM2** | 40 | 1.60 | 5.51 | 431.66 | 77.06 | -6.63 | -10.91 | -59.79 |
| **BMS309403** | 21 | 1.32 | 5.64 | 474.56 | 74.59 | -8.28 | -13.87 | -62.96 |
| **SCPI1** | 350 | 2.54 | 4.53 | 378.28 | 58.05 | -5.64 | -8.93 | -43.99 |
| **SCPI3** | 900 | 2.95 | 2.77 | 364.150 | 86.775 | -6.21 | -8.10 | -40.17 |
| **SCPI4** | 33 | 1.52 | 4.47 | 363.55 | 28.94 | -6.57 | -11.11 | -49.04 |
| **THC** | 1000 | 3.00 | 5.64 | 314.47 | 25.95 | -8.14 | -8.93 | -47.70 |
| **CBD** | 167 | 2.22 | 5.38 | 314.47 | 38.18 | -8.47 | -9.42 | -49.63 |
| **JWH-018** | 58 | 1.76 | 6.17 | 341.45 | 24.03 | -8.25 | -11.40 | -50.87 |

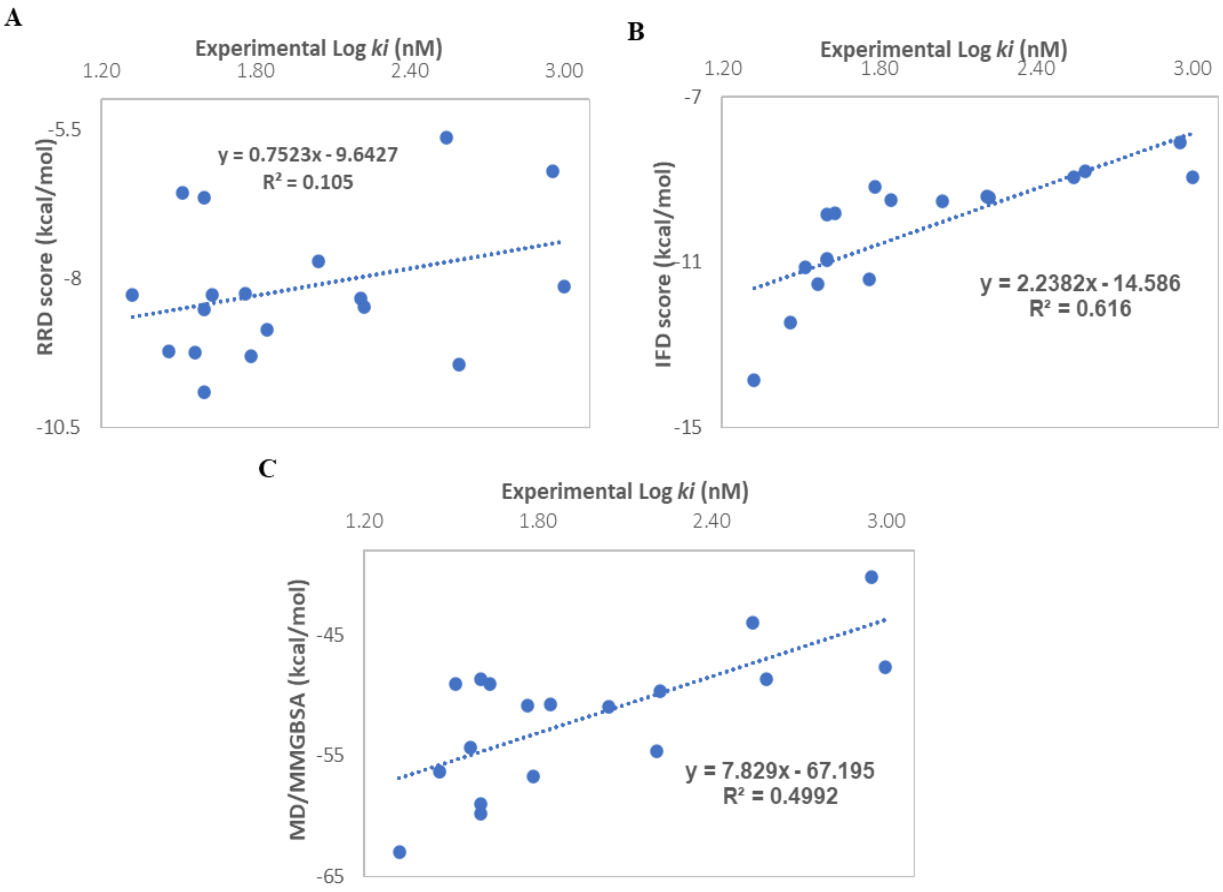


**Figure 3**. Correlation analysis between experimental values, (A) RRD, (B) IFD scores and (C) MD/MM-GBSA in FABP1.

The first effort was simply to plot the correlation between the three methods for predicting binding affinites (rigid docking score, RRD, induced docking score; IFD; and post-MD corrected binding energy, MMGBSA) and the experimental *Ki*. There is only a weak correlation between the experimental log *Ki* and the RRD score ($R^2$ = 0.11, Fig 2A). This however improves markedly when induced-fit docking is used ($R^2$ = 0.62, Fig 2B).[23] This makes sense considering that we expect the binding site to undergo significant rearrangement upon the binding of a ligand. This is true for all proteins of course, but especially true for the FABPs where the "roof" of the binding site closes down over the ligand when it enters the protein. The *apo*-form is interesting as a starting point, but a rigid *apo*-form is unsurprisingly a poor mimic for an occupied FABP.

Rigid docking was never likely to return a useful result. Using MM-GBSA analysis of the MD simulations does result in a decrease in the Pearson coefficient to 0.5. Ideally, we would see a

perfect correlation between experimental and theoretical data, but this is never the case. Experimental data can have significant inherent error, and this can exacerbate differences in the correlation. Another complication is that these are all strong binders. We have nothing above 1 μM in the data set, and this means we cover under two orders of magnitude. This essentially makes them similar binders and it can be difficult to differentiate small changes in affinity using medium-throughput computational methods or experimental methods. A Pearson of 0.6 is perfectly acceptable as a starting point. The quality of the analysis is also hindered by the similarity within classes of these ligands, there is not a large conformational, and hence interaction, variety.

For all the NAE and 2-MG ligands, the oxygen of the amide/arachidonic acid group is predicted to directly interact with $\mathbf{M^{74}}$. All the phenolic AEA uptake inhibitors are predicted to orient towards the inside of the pocket, where the phenolic oxygen would interact with $\mathbf{R^{122}}$ and $\mathbf{S^{124}}$. **SCPI1** & **SCPI3** are predicted to have an interaction with $\mathbf{M^{74}}$, **SCPI4** & **CBD** with $\mathbf{M^{74}}$, and **JWH-013** with $\mathbf{R^{122}}$ (Fig. S1A). These are likely reasonable poses, both because of the match to experimental data and because the IFD docking pose for THC closely reflects the crystallographic result (PDB: *6MP4*, Fig. S1B). This was promising from the simple reorganization of the protein; for a hopefully more accurate reflection of the energies and binding poses, we conducted an MD simulation followed by MMGBSA binding free energy calculations This resulted in an acceptable correlation between the experimental values (log *Ki*(nM)) and the MD/MM-GBSA energies ($R^2$ = 0.50, Fig 2C).

The experimental and computational results both agree that **BMS309403** has the strongest affinity for the target. However, any displacement or functional assay generally relies on factors additional to simple thermodynamic binding between ligand and the protein, and the way the FABP1 assay works suggests that compartmentalization into a lipid membrane might be an important factor in refining the local concentration of the ligand near the protein.[1, 24] However, all attempts to improve correlation with weighted correction terms representing the logP, the molecular weight, or the solubility PlogS do not lead to improvements in $R^2$. Consequently, the raw induced fit binding score is used as the input, and the relaxed *apo*-form of the protein was used as the model structure.

### 3-1. FABP1 and cannabinoids

In this work, a total of 140 cannabinoids were evaluated for their binding with FABP1, including 129 MCs and 11 synthetic cannabinoids. We employed XP RRD with a 0.8 scaling of the van der Waals radii of non-polar atoms for each cannabinoid ligand. After rejecting any pose with root-mean square deviation >2 Å, the highest scored pose for each ligand was advanced to Prime/MM-GBSA analysis to better determine the free energy of the complex (and consequently the binding energy).[22] Table S1 shows the calculated LogP(O/W), total CNS activity, molecular weight (MW), polar surface area (PSA), and calculated RRD and Prime/MM-GBSA values. As noted in our validation study, we expected rigid docking to not provide a good correlation to experiment, so the top 9 RRD-scored MCs, the top 9 Prime/MM-GBSA (excluding duplicates), the two top RRD-scored synthetic cannabinoids, and the biologically important **PA**, **THC**, **CBD**, and **THCA** comprised the 26 total ligands that were advanced to a more computationally expensive IFD analysis (Table 2).

**Table 2.** ADME, RRD scores, Prime/MM–GBSA and IFD and MD/MMGBSA of 26 selected ligands with FABP1.

| Ligand | Physiochemical Properties | | | Computational (kcal/mol) | | | | | | |
|---|---|---|---|---|---|---|---|---|---|---|
| | logPo/w | MW | PSA | RRD 0.8 | Prime MM-GBSA | IFD | Receptor residues interaction | | | MD MM-GBSA |
| | | | | | | | $N^{111}$ | $S^{100}$ | $M^{74}$ | |
| **THC(1)** | 5.71 | 314.47 | 26.61 | -7.58 | -59.77 | -8.93 | √ | --- | --- | -44.07 |
| **THCA(2)** | 5.67 | 358.48 | 70.09 | -8.24 | -41.37 | -9.77 | √ | --- | --- | -35.38 |
| **CBG (29)** | 5.82 | 316.48 | 41.95 | -8.07 | -69.53 | -10.79 | √ | √ | --- | -48.68 |
| **CBGA (30)** | 5.54 | 360.49 | 84.39 | -9.47 | -61.18 | -12.53 | √ | √ | --- | -56.52 |
| **Camagerol_1 (36)** | 4.25 | 350.50 | 81.37 | -9.28 | -69.22 | -11.58 | √ | √ | --- | -39.54 |
| **Sesqui-CBG (39)** | 7.23 | 384.60 | 39.43 | -8.32 | -80.81 | -12.78 | √ | √ | --- | -55.47 |
| **Sesqui-CBGA (39-2)** | 7.62 | 428.61 | 82.92 | -8.02 | -73.17 | -12.69 | √ | √ | --- | -51.52 |
| **(5-acetyl-4-hydroxy-CBG) (40)** | 5.39 | 374.52 | 73.58 | -9.57 | -76.80 | -12.26 | √ | --- | --- | -58.33 |
| **CBC_1 (45)** | 5.85 | 314.47 | 28.83 | -8.22 | -66.00 | -10.96 | √ | √ | --- | -43.24 |
| **CBCVA_1 (48)** | 4.82 | 330.42 | 67.78 | -9.53 | -34.44 | -11.37 | √ | --- | --- | -52.15 |
| **CBD (54)** | 5.29 | 314.47 | 39.36 | -7.5 | -70.53 | -9.42 | --- | √ | --- | -49.63 |
| **ICBT (82)** | 4.07 | 346.47 | 63.12 | -9.24 | -56.95 | -10.07 | √ | √ | --- | -44.23 |
| **ICBT-OET (85)** | 5.12 | 374.52 | 47.90 | -8.58 | -71.39 | -11.26 | --- | √ | √ | -48.43 |
| **CBCN (95)** | 4.14 | 332.44 | 77.01 | -9.43 | -61.05 | -10.56 | √ | √ | √ | -37.39 |
| **CBCON (99)** | 5.02 | 328.45 | 45.81 | -8.76 | -66.88 | -10.87 | √ | --- | √ | -51.4 |
| **CBC-D (107)** | 4.53 | 314.42 | 36.26 | -9.92 | -69.38 | -11.34 | √ | --- | √ | -42.68 |
| **THCP(121)** | 6.50 | 342.52 | 26.63 | -8.73 | -73.97 | -11.56 | √ | √ | √ | -49.51 |
| **Sesqui-THC (124)** | 6.74 | 382.59 | 24.04 | -8.5 | -91.71 | -12.29 | --- | √ | --- | -49.25 |
| **Sesqui-THCA (125)** | 7.01 | 426.60 | 63.82 | -7.97 | -68.58 | -11.74 | --- | √ | --- | -47.87 |
| **Sesqui-THCV (126)** | 6.40 | 354.53 | 24.04 | -7.75 | -85.07 | -12.59 | --- | √ | --- | -51.49 |
| **Sesqui-CBD (127)** | 6.72 | 382.59 | 32.29 | -8.13 | -78.38 | -11.91 | --- | √ | --- | -51.65 |
| **AEA (a1)** | 6.67 | 345.57 | 37.94 | -7.34 | -78.07 | -9.53 | --- | --- | √ | -51.01 |
| **2-AG (a2)** | 6.67 | 378.55 | 74.91 | -8.68 | -84.06 | -9.16 | --- | --- | √ | -56.76 |
| **AM12033 (a7)** | 5.20 | 413.60 | 74.37 | -9.23 | -65.64 | -13.07 | √ | √ | --- | -53.45 |
| **Nabilone (a11)** | 5.52 | 372.55 | 55.75 | -9.89 | -70.04 | -12.37 | √ | √ | --- | -48.39 |
| **PA** | 5.00 | 256.43 | 50.00 | -6.25 | -8.55 | -12.53 | √ | --- | --- | -56.31 |

This analysis shows that, by IFD, many phytocannabinoids are predicted to have meaningful affinity for FABP1, ranging from -8.93 to -18.05 kcal/mol; many of these are predicted to be tighter binders than the designed FABP inhibitors (Table 1), and certainly stronger than the **EC**s (Table 2). All 23 examined cannabinoids have strong interactions with at least one of **N$^{111}$**, **S$^{100}$**, or **M$^{74}$** either directly or through a water-mediated hydrogen bond. This interaction is what makes them strong binders. Hydrophobicity of course also plays a role in determining binding to a fatty-acid binding pocket: as the polarity of the ligand increases, the stronger the desolvation penalty, and consequently the weaker the overall binding within the hydrophobic pocket.[12] Another significant class of binders are the longer chain homologues of the common cannabinoids, the sesquicannabinoids which have a 7-membered alkyl chain on their resorcinol in place of **THC** and **CBD**'s pentyl chain. **Sesqui-CBG** forms a π-cation interaction with **F$^{50}$** and the phenolic hydroxyl groups form H-Bonds with **E$^{72}$**, **S$^{100}$** and **N$^{111}$**. Its long alkyl chain extends deeply into the pocket and forms an L-shape hydrophobic interaction with the base β-sheet floor of FABP1 (Fig. 4A). The major cannabinoids are by far the weakest predicted binders of those investigated: for both **THC** and **CBD** the $O_5$ atom of their ring systems forms H-Bonds with **N$^{111}$**. **CBD** forms a π-cation interaction with **F$^{50}$**, and its phenolic hydroxyl group forms an H-Bond with **S$^{100}$** (Fig. 4B and 4C).

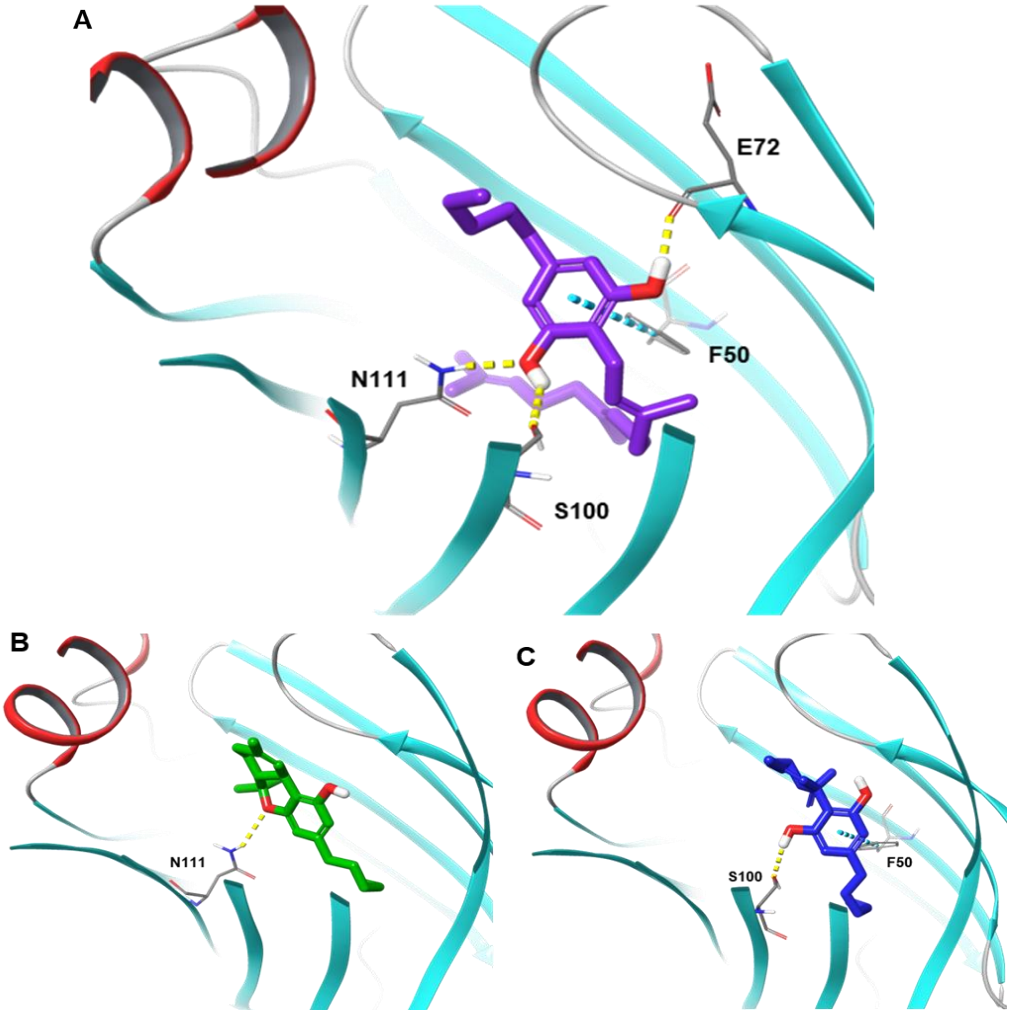


**Figure 4.** IFD binding poses of (A) **Sesqui-CBG** (MD: purple) (B) **THC** (dark green) and (C) **CBD** (dark blue) in complex with FABP1 (PDB ID: *6MP4*). The oxygen atoms are in red and nitrogen in blue, H-bonds in yellow dotted lines, π-cation interaction in dark green dotted lines.

Since the docking scores suggest most of the cannabinoids have acceptable binding scores, and all higher than **THC**, an MD simulation was performed for all the cannabinoids in Table 2 to calculate the MM-GBSA binding energy of ligands to the protein. It is important to note that these values cannot be interpreted as absolute affinities and are most useful as relative values; the MM-GBSA calculations do not necessarily consider entropic effects and often overestimate binding energies significantly. But this has generally been found to be a systematic error meaning the tool is useful to rank binders, if not predict their actual energy of binding.[25]

The first and second ranked MCs **5-acetyl-4-hydroxy-CBG** and **CBGA** have MM-GBSA-predicted binding energies of −58.3 and −56.5 kcal/mol respectively. These are in the range of reference values for the experimental ligands (Figure 3, Table 1). These values are close to that of **BMS309403**, the strongest experimentally validated binder to FABP1 (-63.0 kcal/mol). **5-acetyl-4-hydroxy-CBG** fully occupies the binding site and forces it to close around it, as is typical of FABP binders. The phenolic oxygen directly interacts with **E**$^{72}$, **T**$^{73}$ & **N**$^{111}$ (Fig. 5A). **CBGA**, after MD simulation, moves slightly and its acidic group forms an H-bond with **S**$^{100}$, **T**$^{102}$, & **R**$^{122}$; likewise, its phenolic OH H-bonds with **E**$^{72}$ (Fig. 5B). The MD simulation leads to a complete flip for **THC (Fig S1b)**, its binding is now completely different from that observed by IFD, with its phenolic group now forming H-bond interactions with both **S**$^{100}$ and **N**$^{111}$ (Fig. 5C). Here the phenol is attempting to mimic the hydrogen bond normally formed by a carboxylic acid. It is important to note that it is the IFD structure that aligns with the crystal structure; however, both poses have similar low energies, suggesting both poses are possible. **CBD** only moves very little; its overall structure remains the same as the IFD docking structure, and this also means that it has no specific conserved H-Bond interactions (Fig. 5D). The sesqui-terpene minor cannabinoids maintain good binding energy to FABP1, and are also worthy of further experimental study.

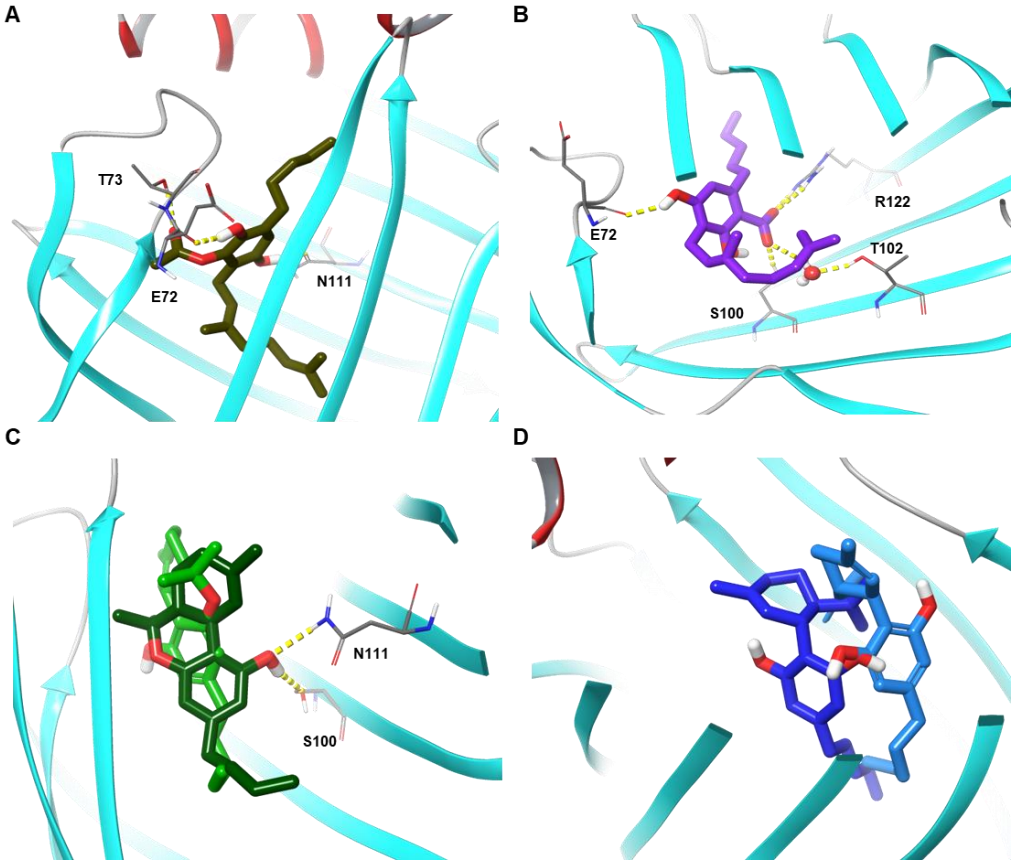


**Figure 5.** The most representative structure of the lowest energy conformation of the complex obtained by clustering of the MD for, (A) **5-acetyl-4-hydroxy-CBG** (brown) (B) **CBGA** (MD: purple) (C) **THC** (dark green) and (D) **CBD** (dark blue) in complex with FABP1 (PDB ID: *6MP4*). The oxygen atoms are in red, nitrogen is in blue, and H-bonds are represented yellow dotted lines.

To validate the stability of the ligand binding mode in the complexes, RMSD of the backbone atoms relative to first frame of the MD simulation were calculated for the first 100 ns (Fig. 6A). All complex structures reached equilibrium after no more than 16 ns. The average RMSD value calculated for FABP1 in complex with **5-acetyl-4-hydroxy-CBG**, **CBGA**, **CBD**, **THC**, **PA**, two molecules of **PA**, **AEA**, **2GA** and apo protein were 1.74, 1.77, 1.94, 1.63, 1.74, 2.07, 2.01, 1.99 and 1.92 angstrom respectively. These reasonable RMSD values strongly imply the complex remains largely stable. These don't meaningfully suggest major differences between the ligands with the possible suggestion that the phytocannabinoids restrict overall motion more than either the ECs or the FAs. However, the RMSD, being calculated over the entire complex can

mask substantial flexibility in some components, or can overstate the movement of other components.

Consequently, per residue root mean square fluctuations (RMSFs) of the protein backbone in FABP1 were calculated (Fig 6B). The protein clearly, in general, becomes less flexible when a ligand is bound, particularly in the portal region, which is composed of α helix 2, β turn CD, and β turn EF (Figure 6C). **CBGA**, **5-acetyl-4-hydroxy-CBG**, **THC** and **CBD** reduced the flexibility of α helix 2. Of all the ligands examined, **CBGA** and **THC** are the most effective in reducing the flexibility of α helix 2. β-turn EF also becomes stabilized upon binding the ligands. This reduction in flexibility of these motifs is consistent with the observed interactions of the ligands with **E**$^{72}$, **T**$^{73}$, **R**$^{122}$, **S**$^{100}$ and **N**$^{111}$. Interaction locks them into place relative to one another, and would be expected to reduce their motion, and consequently that of their parent secondary motif.

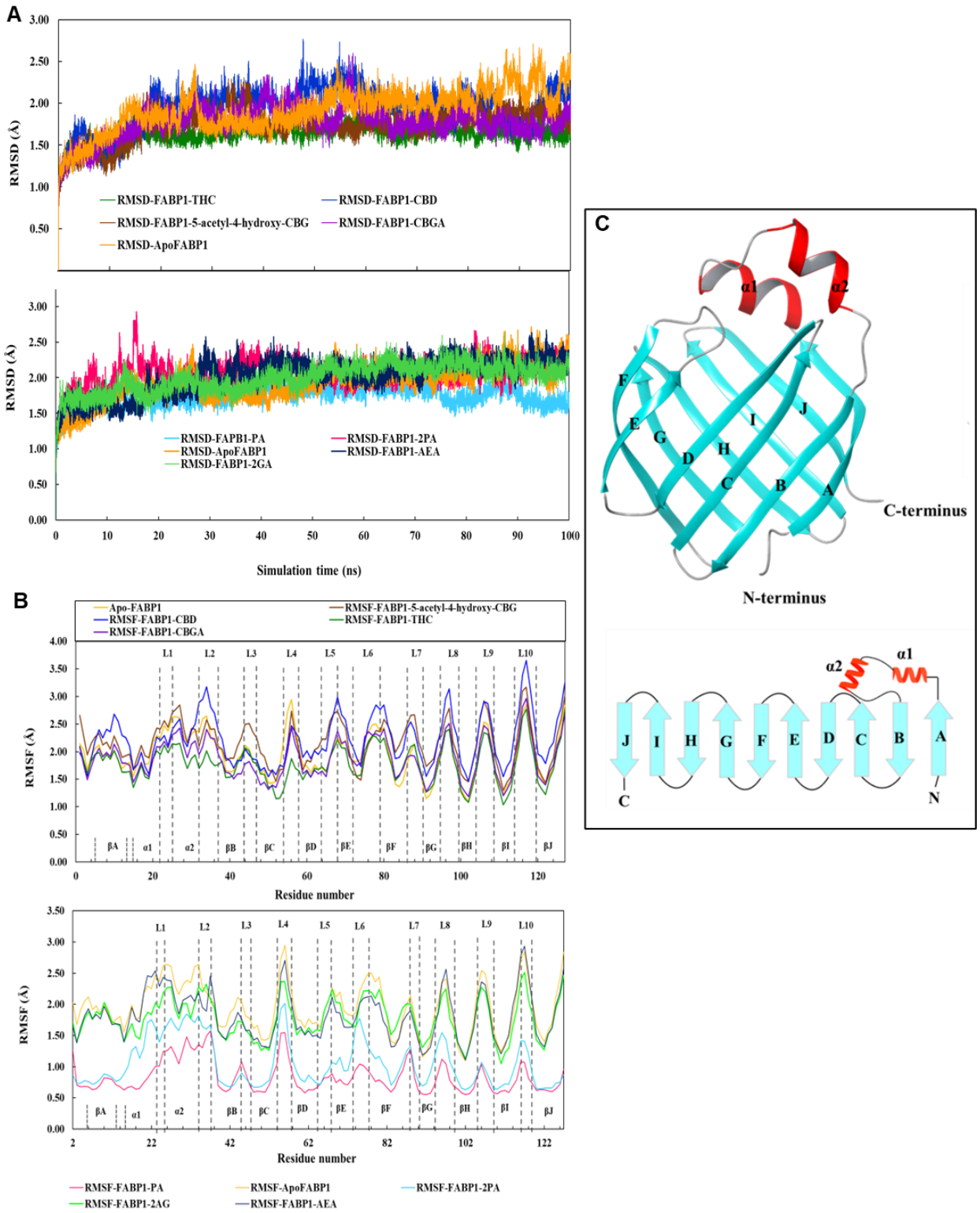


**Figure 6.** A) Root-mean-square deviations (RMSD) and B) Root mean square fluctuations (RMSFs) of backbone atoms relative to their initial minimized structures as function of time for FABP1.

However, the greatest reduction in flexibility occurs when the endogenous ligand **PA** binds. The reduction in flexibility is even greater when two molecules of **PA** bind to the cavity. The effect is strongest at α helix 2, β turn CD, and β turn EF. These are the same motifs affected by the ECs and MCs. This effect is likely driven by the conserved hydrogen bonds between the **PA**s and key residues **R$^{122}$**, **S$^{39}$** and **S$^{124}$** (Table 3). The same, although lesser, decreased flexibility of the portal region is observed upon binding of the natural ECs **2-AG** and **AEA**. Analysis of hydrogen bonds between these ligands and FABP1 revealed that **E$^{72}$** and **M$^{74}$** created a hydrogen bond with **2-AG** which may result in reduction of flexibility in portal region of protein. However, no hydrogen bonds between **AEA** and any residues of FABP1 was detected. Comparing hydrogen bonds pattern between ligands in FABP1 in complex with ECs and **CBGA** and **5-acetyl-4-hydroxy-CBG** revealed that the hydrogen bond between ligands and **E$^{72}$** become more stable (Table 3).

**Table 3.** Hydrogen bonds formed between the ligands and FABP1.

| Ligand | Donor | Acceptor | Average Distance (Å) | %Occupancy |
|---|---|---|---|---|
| **5-acetyl-4-hydroxy-CBG** | 5-acetyl-4-hydroxy-CBG@O2 | E$^{72}$@O | 2.77 | 60.58 |
| | T$^{73}$@OG1 | 5-acetyl-4-hydroxy-CBG@O4 | 2.76 | 26.5 |
| | 5-acetyl-4-hydroxy-CBG@O1 | N$^{111}$@OD1 | 2.75 | 23.66 |
| | N$^{111}$@ND2 | 5-acetyl-4-hydroxy-CBG@O1 | 2.87 | 17.35 |
| **CBGA** | R$^{122}$@NH2 | CBGA@O4 | 2.83 | 63.3 |
| | CBGA@O1 | E$^{72}$@O | 2.76 | 61.78 |
| | R$^{122}$@NH1 | CBGA@O4 | 2.78 | 50.83 |
| | R$^{122}$@NH1 | CBGA@O3 | 2.77 | 41.56 |
| | S$^{100}$@OG | CBGA@O3 | 2.61 | 41.45 |
| | R$^{122}$@NH2 | CBGA@O3 | 2.81 | 33.74 |
| | CBGA@O2 | S$^{100}$@OG | 2.8 | 25.09 |
| **THC** | THC @O2 | E$^{72}$@O | 2.73 | 86.6 |
| **PA** | R$^{122}$@NH2 | PA@O1 | 2.79 | 76.5 |
| | S$^{39}$@OG | PA@O1 | 2.63 | 73.42 |
| | R$^{122}$@NE | PA@O2 | 2.82 | 63.3 |
| | S$^{124}$@OG | PA@O2 | 2.69 | 57.21 |
| | R$^{122}$@NH2 | PA@O2 | 2.83 | 31.1 |
| | S$^{39}$@OG | PA@O2 | 2.61 | 17.01 |
| | R$^{122}$@NE | PA@O1 | 2.81 | 16.99 |
| | S$^{124}$@OG | PA@O1 | 2.72 | 14.75 |
| **2PA** | R$^{122}$@NH2 | PA2*@O1 | 2.76 | 67.4 |
| | S$^{39}$@OG | PA1*@O2 | 2.68 | 57.3 |

| | | | | |
|---|---|---|---|---|
| | $R^{122}$@NH1 | PA1@O1 | 2.8 | 51.12 |
| | $R^{122}$@NH2 | PA1@O2 | 2.8 | 43.66 |
| | $S^{124}$@OG | PA1@O1 | 2.67 | 40.84 |
| | $S^{100}$@OG | PA2@O2 | 2.62 | 40.17 |
| | $R^{122}$@NH1 | PA1@O2 | 2.8 | 39.65 |
| | $R^{122}$@NH2 | PA1@O1 | 2.7 | 38.09 |
| | $S^{39}$@OG | PA1@O1 | 2.66 | 34.5 |
| | $R^{122}$@NH2 | PA2@O2 | 2.78 | 22.7 |
| | $R^{122}$@NE | PA2@O2 | 2.81 | 21.93 |
| | $R^{122}$@NE | PA2@O1 | 2.83 | 19.54 |
| | $N^{111}$@ND2 | PA2@O1 | 2.8 | 15.44 |
| | $S^{124}$@OG | PA1@O2 | 2.66 | 14.67 |
| **2-AG** | $M^{74}$@N | 2-AG@O4 | 2.87 | 34.61 |
| | 2-AG@O2 | $E^{72}$@O | 2.74 | 14.92 |
| **AEA** | --- | --- | --- | --- |

* PA1 and PA2 are first and second molecules of PA

It is curious that such structurally diverse molecules can show similar high affinity for a protein like FABP1.[26] Computational techniques can help us to evaluate molecular similarity. These techniques can be categorized into three methods; in the first method we can conduct QSAR analyses comparing chemical and molecular properties such as lipophilicity (logPo/w), molecular weight (MW) and polar surface area (PSA) of FAs, synthetic ligands, ECs and MCs. Using this approach reveals no significant trends between these parameters and either experimental binding affinity, or computationally calculated IFD or MD/MM-GBSA values. The second method, employing the Tanimoto similarity measure (which provides a coefficient, *Tc*, between 1 to 0) is common in 2D SAR approaches.[27] According to this analysis, **PA** is more similar to the ECs (0.4 similarity between PA and 2-AG) with far less similarity to the MCs (0.13 similarity between PA and CBD). If one was to use these parameters to predict binding to the protein, one would be sorely mistaken: molecules that are structurally dissimilar tend to bind in a dissimilar fashion, and therefore tend to induce different bioactivities. The important words in that sentence are, of course "tend," and caution must be taken whenever one abstracts a molecule for analysis. A third abstracting approach is the use of interaction fingerprints (IFP) on the bound structure: identifying the residues involved in strong interactions with a given ligand. The key residues identified by an IFP analysis of the FAs binding to FABP1 are **$R^{122}$**, **$N^{111}$**, **$S^{100}$** and **$M^{74}$**. The ECs have very little IFP similarity, but the MCs **5-acetyl-4-hydroxy-CBG** and **GBGA** do share the same residues and have a good IFD match to the FAs (Table 3). However, this type of analysis only works if you

have structural data or a good all atomic simulation. We cannot recommend using any of these approaches to interpret the interactions between the ligands and the receptor, and we strongly recommend that any computational screening technique take all-atomic modelling into account to make any meaningful predictions.

## Conclusion

What is clear from this data is that the ECs can avail themselves of the same transport mechanisms as the FAs. This is well established. The major cannabinoids are known to bind to FABP1, and this activity has been suggested to be responsible for some of their biological activity. However, we show that the strongest affinities likely arise from the interaction of minor cannabinoids with the FABPs. Of course, they are present in lower amounts than THC or CBD, but if one were looking to design an FABP1-inhibiting drug, the minor cannabinoids are likely a better starting point than the major cannabinoids.

Most curiously is that this study provides additional evidence that the PCs imitate the preferred accessible conformation of the ECs. Razdan in 1996,[28] and Howlett in 1998[29] both discussed the pharmacophores of the PCs and ECs, and research since then has tried to combine these two systems into simple cannabinoid receptor agonists and antagonists.[15] However, this similarity is clearly more general and applies to their interactions with other proteins as well. As both we and these authors note, the constrained ring system of the PCs "pays" the entropic cost of binding in a specific conformation up front, increasing binding affinity. This has been clearly discussed in the context of the cannabinoid receptors, but we believe this is the first report suggesting the effect is more general and likely applies to other proteins as well. The effect is also clearly not unique to the ECs. The PCs can imitate far more ubiquitous FAs. Examining other proteins that interact with FAs might prove to be a promising avenue of research to further understand the complex pharmacology of the PCs. Some of this work is currently underway in our lab and will be reported on in due course.

## Supplementary Information and Data Availability:

The supplementary information that accompanies this article includes a more detailed discussion of the computational methodology used to generate the data, complete tables for the rigid binding data for all 131 cannabinoids examined in the article, and 2D interaction plots for FABP1's

endogenous and designer ligands highlighting key interactions. All of the computational input and output geometries, and the required information to recreate the MD trajectories, and consequently all the data in the article, is available from the Borealis repository at: https://doi.org/10.5683/SP3/9HCGOM. This also includes the *apo*-FABP1 structure we use as the basis of our model should anyone wish to use it for further drug discovery work. The Borealis repository is a collaboration of the Canadian Universities to facilitate access to research data.

**Author Credit Statement:**

Conceptualization, JFT, FS; Funding acquisition JFT; Investigation, FS, SM, DM, VA, VT; Methodology, FS, SM, DM, JFT; Visualization, FS, SM; Project administration, JFT; Supervision, JFT, FS; Writing—original draft, FS; Writing—review and editing, All authors.

**Acknowledgements:**

The authors gratefully acknowledge financial support for the project from the Natural Sciences and Engineering Research Council of Canada (JFT: grant # 2018-06338). All authors wish to recognize that this work was made possible by the facilities of the Shared Hierarchical Academic Research Computing Network (SHARCNET: www.sharcnet.ca) and Compute/Calcul Canada, now known as the Digital Alliance of Canada (https://alliancecan.ca/en).

**References**

1. Storch, J.; McDermott, L., Structural and functional analysis of fatty acid-binding proteins. *J. Lipid Res.* **2009,** *50 Suppl* (Suppl), S126-31.
2. Atshaves, B. P.; Martin, G. G.; Hostetler, H. A.; McIntosh, A. L.; Kier, A. B.; Schroeder, F., Liver fatty acid-binding protein and obesity. *J. Nutr. Biochem.* **2010,** *21* (11), 1015-1032.
3. Wang, G.; Bonkovsky, H. L.; de Lemos, A.; Burczynski, F. J., Recent insights into the biological functions of liver fatty acid binding protein 1. *J. Lipid Res.* **2015,** *56* (12), 2238-2247.
4. Hirowatari, K.; Kawano, N., Association of urinary liver-type fatty acid-binding protein with renal functions and antihyperglycemic drug use in type 2 diabetic nephropathy patients. *Int. J. Urol. Nephrol.* **2023**.
5. Martin, G. G.; Atshaves, B. P.; McIntosh, A. L.; Mackie, J. T.; Kier, A. B.; Schroeder, F., Liver fatty acid binding protein gene ablation potentiates hepatic cholesterol accumulation in cholesterol-fed female mice. *Am. J. Physiol. Gastrointest. Liver Physiol.* **2006,** *290* (1), G36-G48.
6. (a) Wu, Y. L.; Peng, X. E.; Zhu, Y. B.; Yan, X. L.; Chen, W. N.; Lin, X., Hepatitis B virus X protein induces hepatic steatosis by enhancing the expression of liver fatty acid binding protein. *J. Virol.* **2016,** *90* (4), 1729-40; (b) Pi, H.; Liu, M.; Xi, Y.; Chen, M.; Tian, L.; Xie, J.; Chen, M.;

Wang, Z.; Yang, M.; Yu, Z.; Zhou, Z.; Gao, F., Long-term exercise prevents hepatic steatosis: A novel role of FABP1 in regulation of autophagy-lysosomal machinery. *FASEB J.* **2019,** *33* (11), 11870-11883.
7. McKillop, I. H.; Girardi, C. A.; Thompson, K. J., Role of fatty acid binding proteins (FABPs) in cancer development and progression. *Cell. Signalling* **2019,** *62*, 109336.
8. Sharma, A.; Sharma, A., Fatty acid induced remodeling within the human liver fatty acid-binding protein. *J. Biol. Chem.* **2011,** *286* (36), 31924-31928.
9. Chuang, S.; Velkov, T.; Horne, J.; Wielens, J.; Chalmers, D. K.; Porter, C. J. H.; Scanlon, M. J., Probing the fibrate binding specificity of rat liver fatty acid binding protein. *J. Med. Chem.* **2009,** *52* (17), 5344-5355.
10. Chuang, S.; Velkov, T.; Horne, J.; Porter, C. J. H.; Scanlon, M. J., Characterization of the drug binding specificity of rat liver fatty acid binding protein. *J. Med. Chem.* **2008,** *51* (13), 3755-3764.
11. Richieri, G. V.; Ogata, R. T.; Kleinfeld, A. M., Equilibrium constants for the binding of fatty acids with fatty acid-binding proteins from adipocyte, intestine, heart, and liver measured with the fluorescent probe ADIFAB. *J. Biol. Chem.* **1994,** *269* (39), 23918-30.
12. Elmes, M. W.; Prentis, L. E.; McGoldrick, L. L.; Giuliano, C. J.; Sweeney, J. M.; Joseph, O. M.; Che, J.; Carbonetti, G. S.; Studholme, K.; Deutsch, D. G.; Rizzo, R. C.; Glynn, S. E.; Kaczocha, M., FABP1 controls hepatic transport and biotransformation of Δ9-THC. *Sci. Rep.* **2019,** *9* (1), 7588.
13. Shahbazi, F.; Grandi, V.; Banerjee, A.; Trant, J. F., Cannabinoids and cannabinoid receptors: The story so far. *iScience* **2020,** *23* (7), 101301.
14. Martin, G. G.; Chung, S.; Landrock, D.; Landrock, K. K.; Huang, H.; Dangott, L. J.; Peng, X.; Kaczocha, M.; Seeger, D. R.; Murphy, E. J.; Golovko, M. Y.; Kier, A. B.; Schroeder, F., FABP-1 gene ablation impacts brain endocannabinoid system in male mice. *J. Neurochem.* **2016,** *138* (3), 407-22.
15. Chen, J.-Z.; Han, X.-W.; Xie, X.-Q., Preferred conformations of endogenous cannabinoid ligand anandamide. *Life Sci.* **2005,** *76* (18), 2053-2069.
16. Citti, C.; Braghiroli, D.; Vandelli, M. A.; Cannazza, G., Pharmaceutical and biomedical analysis of cannabinoids: A critical review. *J. Pharm. Biomed. Anal.* **2018,** *147*, 565-579.
17. Wolfrum, C.; Borrmann, C. M.; Borchers, T.; Spener, F., Fatty acids and hypolipidemic drugs regulate peroxisome proliferator-activated receptors alpha - and gamma-mediated gene expression via liver fatty acid binding protein: a signaling path to the nucleus. *Proc. Natl. Acad. Sci. U. S. A.* **2001,** *98* (5), 2323-8.
18. Tahir, M. N.; Shahbazi, F.; Rondeau-Gagné, S.; Trant, J. F., The biosynthesis of the cannabinoids. *J. Cannab. Res.* **2021,** *3*, 7 (Article Number).
19. Felletti, S.; Compagnin, G.; Krauke, Y.; Stephan, S.; Greco, G.; Buratti, A.; Chenet, T.; De Luca, C.; Catani, M.; Cavazzini, A., Purification and isolation of cannabinoids: Current challenges and perspectives. *LCGC Europe* **2023,** *36* (04), 122–131.
20. Huang, H.; McIntosh, A. L.; Martin, G. G.; Landrock, D.; Chung, S.; Landrock, K. K.; Dangott, L. J.; Li, S.; Kier, A. B.; Schroeder, F., FABP1: A novel hepatic endocannabinoid and cannabinoid binding protein. *Biochemistry* **2016,** *55* (37), 5243-5255.
21. Halgren, T. A.; Murphy, R. B.; Friesner, R. A.; Beard, H. S.; Frye, L. L.; Pollard, W. T.; Banks, J. L., Glide: A new approach for rapid, accurate docking and scoring. 2. Enrichment factors in database screening. *J. Med. Chem.* **2004,** *47* (7), 1750-9.

22. Lyne, P. D.; Lamb, M. L.; Saeh, J. C., Accurate prediction of the relative potencies of members of a series of kinase inhibitors using molecular docking and MM-GBSA scoring. *J. Med. Chem.* **2006,** *49* (16), 4805-8.
23. Zhong, H.; Tran, L. M.; Stang, J. L., Induced-fit docking studies of the active and inactive states of protein tyrosine kinases. *J. Mol. Graphics Modell.* **2009,** *28* (4), 336-346.
24. Velkov, T.; Chuang, S.; Wielens, J.; Sakellaris, H.; Charman, W. N.; Porter, C. J. H.; Scanlon, M. J., The interaction of lipophilic drugs with intestinal fatty acid-binding protein. *J. Biol. Chem.* **2005,** *280* (18), 17769-17776.
25. (a) Hou, T.; Wang, J.; Li, Y.; Wang, W., Assessing the performance of the MM/PBSA and MM/GBSA Methods. 1. The accuracy of binding free energy calculations based on molecular dynamics simulations. *J. Chem. Inf. Model.* **2011,** *51* (1), 69-82; (b) Hou, T.; Wang, J.; Li, Y.; Wang, W., Assessing the performance of the molecular mechanics/Poisson Boltzmann surface area and molecular mechanics/generalized Born surface area methods. II. The accuracy of ranking poses generated from docking. *J. Comp. Chem.* **2011,** *32* (5), 866-877; (c) Rastelli, G.; Rio, A. D.; Degliesposti, G.; Sgobba, M., Fast and accurate predictions of binding free energies using MM-PBSA and MM-GBSA. *J. Comp. Chem.* **2010,** *31* (4), 797-810.
26. Xu, X.; Zou, X. Dissimilar ligands bind in a similar fashion: A guide to ligand binding-mode prediction with application to CELPP studies *Int. J. Mol. Sci.* [Online], 2021.
27. Bajusz, D.; Rácz, A.; Héberger, K., Why is Tanimoto index an appropriate choice for fingerprint-based similarity calculations? *J. Cheminform.* **2015,** *7* (1), 20.
28. Thomas, B. F.; Adams, I. B.; Mascarella, S. W.; Martin, B. R.; Razdan, R. K., Structure−activity analysis of anandamide analogs: Relationship to a cannabinoid pharmacophore. *J. Med. Chem.* **1996,** *39* (2), 471-479.
29. Tong, W.; Collantes, E. R.; Welsh, W. J.; Berglund, B. A.; Howlett, A. C., Derivation of a pharmacophore model for anandamide using constrained conformational searching and comparative molecular field analysis. *J. Med. Chem.* **1998,** *41* (22), 4207-4215.